frontiers in Energy Research

ORIGINAL RESEARCH
published: 16 March 2015
doi: 10.3389/fenrg.2015.00012

The marine microalga, *Heterosigma akashiwo*, converts industrial waste gases into valuable biomass

Jennifer J. Stewart[1]*, *Colleen M. Bianco*[2], *Katherine R. Miller*[3] and *Kathryn J. Coyne*[1]

[1] College of Earth, Ocean, and Environment, University of Delaware, Lewes, DE, USA, [2] Department of Microbiology, University of Illinois at Urbana-Champaign, Urbana, IL, USA [3] Department of Chemistry, Salisbury University, Salisbury, MD, USA

Heterosigma akashiwo is an excellent candidate for growth on industrial emissions since this alga has the ability to metabolize gaseous nitric oxide (NO) into cellular nitrogen via a novel chimeric protein (NR2-2/2HbN) and also tolerates wide fluctuations in temperature, salinity, and nutrient conditions. Here, we evaluated biomass productivity and composition, photosynthetic efficiency, and expression of *NR2-2/2HbN* for *Heterosigma* growing on simulated flue gas containing 12% CO_2 and 150 ppm NO. Biomass productivity of *Heterosigma* more than doubled in flue gas conditions compared to controls, reflecting a 13-fold increase in carbohydrate and a 2-fold increase in protein productivity. Lipid productivity was not affected by flue gas and the valuable omega-3 fatty acids, eicosapentaenoic acid and docosahexaenoic acid, constituted up to 16% of total fatty acid methyl esters. Photochemical measurements indicated that photosynthesis in *Heterosigma* is not inhibited by high CO_2 and NO concentrations, and increases in individual fatty acids in response to flue gas were driven by photosynthetic requirements. Growth rates and maximum cell densities of *Heterosigma* grown on simulated flue gas without supplemental nitrogen, along with a significant increase in *NR2-2/2HbN* transcript abundance in response to flue gas, demonstrated that nitrogen derived from NO gas is biologically available to support enhanced CO_2 fixation. Together, these results illustrate the robustness of this alga for commercial-scale biomass production and bioremediation of industrial emissions.

Keywords: bioremediation, biofuel, algae, carbon dioxide, nitric oxide, raphidophyte, biomass

OPEN ACCESS

Edited by:
Umakanta Jena, Desert Research Institute, USA

Reviewed by:
Alberto Scoma, Ghent University, Belgium
Probir Das, Qatar University, Qatar
Liz M. Diaz, University of Puerto Rico, USA

***Correspondence:**
Jennifer J. Stewart, College of Earth, Ocean, and Environment, University of Delaware, 700 Pilottown Road, Lewes, DE 19958, USA
jen@udel.edu

Specialty section:
This article was submitted to Bioenergy and Biofuels, a section of the journal Frontiers in Energy Research

Received: *03 December 2014*
Accepted: *26 February 2015*
Published: *16 March 2015*

Citation:
Stewart JJ, Bianco CM, Miller KR and Coyne KJ (2015) The marine microalga, Heterosigma akashiwo, converts industrial waste gases into valuable biomass. Front. Energy Res. 3:12. doi: 10.3389/fenrg.2015.00012

Introduction

The globally distributed algal species *Heterosigma akashiwo* (Y. Hada) Y. Hada ex Y. Hara & M. Chihara (Hara and Chihara, 1987) is a unicellular chromophyte alga within the class Raphidophyceae and is well known for forming dense blooms in coastal and estuarine systems worldwide (Zhang et al., 2006; Martínez et al., 2010). *Heterosigma* has been identified as a promising candidate for the production of high quality biodiesel and is capable of achieving a higher total lipid content than several other microalgal species traditionally used in biodiesel production (Fuentes-Grünewald et al., 2013; 2012; 2009). This robust organism tolerates wide fluctuations in temperature, salinity, and nutrient conditions (Martínez et al., 2010), suggesting that this alga would be a viable option for commercial-scale biomass production. *Heterosigma* is also an excellent candidate for growth on industrial emissions (i.e., "flue gases"), since this alga has the ability to metabolize gaseous NO into cellular nitrogen via a novel chimeric protein, NR2-2/2HbN (Stewart and Coyne, 2011).

Developing innovative CO_2 utilization strategies is essential for overcoming the barriers to economic and sustainable algal biomass production, since CO_2 supplementation is a requirement for commercial biomass production due to carbon limitation at atmospheric CO_2 levels (Benemann, 2013). Utilizing flue gas CO_2 would have the dual advantage of simultaneously decreasing biomass production costs while also mitigating the effects of harmful greenhouse gas emissions. CO_2 accounts for 82% of anthropogenically derived greenhouse gas emissions in the United States (EPA, 2012), and it is widely accepted that remediation of CO_2 emissions is essential for mitigating global climate change. In addition, flue gas also contains cytotoxic nitrogen oxides (NOx, > 90% as nitric oxide), and the reaction products of NOx emissions, ozone (O_3) and nitrous oxide (N_2O), are also potent greenhouse gases (EPA, 2014). Harnessing both CO_2 and NOx emissions from flue gas as nutrient sources for *Heterosigma* growth could theoretically reduce operating costs for biomass production by 50% (Douskova et al., 2009; Nagarajan et al., 2013).

Utilization of industrial CO_2 for algal growth has been investigated for a variety of algal species, including *Spirulina* sp. (Chen et al., 2012), *Chlorella* sp. (Doucha et al., 2005; Douskova et al., 2009; Borkenstein et al., 2011; Chiu et al., 2011), and *Dunaliella* sp. (Harter et al., 2013). The green alga, *Scenedesmus* sp., is able to grow in high CO_2 and NOx environments and is currently being evaluated for growth on industrial emissions (Jin et al., 2008; Santiago et al., 2010; Basu et al., 2013; Jiang et al., 2013; Lara-Gil et al., 2014; Wilson et al., 2014). Continued identification and characterization of algal species that thrive in these harsh conditions is a critical step toward economically viable production of algal biofuels and bioproducts. To address this critical research gap, we evaluated biomass productivity, cellular composition, photosynthetic efficiency, and expression of *NR2-2/2HbN* for *H. akashiwo* growing on simulated flue gas containing 12% CO_2 and 150 ppm NO. Results of this work will support the development of commercial platforms for cultivating algal biomass on flue gas for the biofuels and bioproducts industries.

Materials and Methods

Strains and Experimental Culture Conditions

H. akashiwo CCMP 2393 (NCMA; Boothbay Harbor, ME, USA) was maintained in seawater diluted to a salinity of 20 ppt and amended with f/2 nutrients (-Si) (Guillard, 1975), buffered with 20 mM HEPES (pH = 7.35), and grown at room temperature and an irradiance of ~80 µmol quanta m^{-2} s^{-1} on a 12:12 h light:dark cycle. Light provided by cool white fluorescent bulbs was measured using an LI-250A light meter (LI-COR Biosciences, Lincoln, NE, USA) placed against the external wall of the culture vessel at a point closest to the light source. Cultures were grown in 1 L narrow-mouth polycarbonate bottles (diameter = 99 mm; Thermo Fisher Scientific, Waltham, MA, USA) sealed with screw caps retrofitted with inlet and outlet ports attached to PTFE tubing (3/16″ ID, 1/4″ OD, 1/32″ wall). Cultures were bubbled continuously (2 mL min^{-1}) with compressed air (control) or a simulated flue gas mixture consisting of 12% CO_2 and 150 ppm NO balanced in N_2 through rigid PTFE tubing that extended to the bottom of the vessel. The headspace was vented through a short piece of PTFE tubing stuffed with cotton fitted to the outlet port.

Cultures were maintained in batch growth under experimental conditions for five cycles (35 days) by replacing culture with fresh media every 7 days to achieve an initial density of 180,000 cells/mL at the start of each batch cycle. During the sixth cycle, replicate cultures (500 mL; $n = 4$) were sampled during mid-log growth for analysis of total carbohydrate, protein and lipid content, lipid profiles, gene expression, seawater chemistry, particulate carbon and nitrogen, and photochemistry as described below.

In a separate experiment, cells acclimated to growth on either air or simulated flue gas for five cycles were used to seed replicate cultures (500 mL; $n = 4$) and cultivated in modified f/2 media containing either 0 or 220 µM sodium nitrate ($NaNO_3$). Growth was monitored daily for 12 days using an improved neubauer hemocytometer (Thermo Fisher Scientific) to calculate cell density. Specific growth rate (µ) was calculated using the following equation:

$$\mu = [\mathrm{Ln}\,(N_2 \div N_1)] \div (t_2 - t_1) \quad (1)$$

where N_2 and N_1 are cell densities (cells/mL) at t_2 and t_1, respectively.

Cell Counts, Cell Size, and Cell Weight

Cell counts and cell sizes were determined using a Multisizer 3 Coulter Counter (Beckman Coulter, Indianapolis, IN, USA). Dry weight (DW) was determined from a calibration curve of DW (mg/L) versus cell counts (cells/mL) of serially diluted *H. akashiwo* harvested during exponential growth. Specifically, triplicate samples of each dilution were filtered onto pre-combusted and pre-weighed GF/F glass fiber filters (Whatman/GE Lifesciences, Pittsburg, PA, USA) and washed with 0.5 M ammonium bicarbonate to remove salts. Samples were dried at 90°C to constant weight to obtain DW. Cell concentrations (cells/mL) obtained during the experiment were then converted to DW (mg/L) equivalents. Volumetric productivity (mg L^{-1} day^{-1}) for biomass and biochemical constituents was calculated using the following equation:

$$\mathrm{Productivity} = (N_2 - N_1) \div (t_2 - t_1) \quad (2)$$

where N_2 and N_1 are biomass or biochemical constituent concentrations (mg L^{-1}) at t_2 and t_1, respectively.

Carbon Chemistry

Culture samples were collected in glass vials fitted with conical caps, preserved with 5% $HgCl_2$, and stored at 4°C until analysis. Dissolved inorganic carbon (DIC) was determined by the method of Sharp et al. (2009) using a custom built acid sparging instrument described in Friederich et al. (2002) fitted with a high precision flow control infrared analyzer (LI-COR Biosciences). Partial pressure of CO_2 was calculated from DIC and pH using the CO_2calc application version 1.0.3. Calculations were preformed using the GEOSECS (Li et al., 1969) option for acidity constants, the borate acidity constant of Dickson (1990), and the seawater pH scale.

Expression of *NR2-2/2HbN*

Cultures were filtered on 3-μm polycarbonate membrane filters and immediately submerged in Buffer RLT (Qiagen, Germantown, MD, USA) for gene expression analysis. Total RNA was extracted using the RNEasy Plant Mini Kit (Qiagen) and resuspended in RNase-free water. The purity of total RNA was analyzed spectroscopically (Nanodrop, Thermo Fisher Scientific) and RNA was treated with DNase I (Invitrogen/Life Technologies, Grand Island, NY, USA) as previously described (Coyne and Cary, 2005). Approximately 1 μg of DNase-treated total RNA was reverse transcribed with oligodT primer using the Superscript III First Strand Synthesis System (Invitrogen). Duplicate reactions for each DNase-treated RNA sample without reverse transcriptase were also evaluated by PCR. Transcript abundances for nitrate reductase (NR2-2/2HbN) and glyceraldehyde 3-phosphate dehydrogenase (HaGAP, as a reference gene) were determined by quantitative real time-PCR using the Stratagene MX3005P Sequence Detection System (Agilent Technologies, Santa Clara, CA, USA) as previously described (Stewart and Coyne, 2011).

Total Lipid, Protein, and Carbohydrate Quantification

Culture was centrifuged for 5 min at 4000 RPM using a swinging bucket rotor centrifuge (Thermo Fisher Scientific). Total lipid content was determined using the colorimetric sulfo-phospho-vanillin assay for microalgae as described by Cheng et al. (2011) and optimized during this study for *H. akashiwo*. Lipids were extracted from centrifuged algal cells using the method developed by Folch et al. (1957). Briefly, the frozen algal pellet was homogenized with a 2:1 chloroform-methanol mixture then washed with 0.2 volumes of 0.05 M NaCl in deionized water, making a final critical ratio of 2:1:0.8 chloroform-methanol-sodium chloride solution. For the assay, 100 μL of the lower phase containing the pure lipid extract or corn oil standards containing 5–160 μg lipids in chloroform were added directly to a 96-well PCR plate. Methanol was added to each well to obtain a 2:1 chloroform-methanol ratio. The solvent was evaporated by placing the plate in a warm water bath, and then 100 μL of concentrated sulfuric acid was added to each well. The plate was then incubated at 90°C for 20 min and cooled on ice for 2 min. Equal volumes of samples and standards were transferred to a 96-well polypropylene microplate (Costar, Corning Life Sciences, Tewksbury, MA, USA) and background absorbance was measured at 540 nm. Vanillin-phosphoric acid reagent (0.2 mg/mL vanillin in 17% phosphoric acid) was immediately added to obtain a final vanillin concentration of 0.06 mg/mL. After 5 min of color development, the absorbance was measured at 540 nm on an Omega Star Microplate Reader (BMG LABTECH, Ortenburg, Germany) and total lipid content was determined by linear regression using corn oil standards.

Proteins were extracted from the centrifuged algal cells by sonication in 200 mM potassium phosphate buffer. Total protein was measured using the BCA Protein Assay Kit (Pierce, Rockford, IL, USA) according to manufacturer instructions and protein content was determined by linear regression analysis.

Carbohydrate content was determined using the phenol-sulfuric acid colorimetric method described by Dubois et al. (1956). Centrifuged algal cells were re-suspended in deionized water, and phenol and sulfuric acid were added to give a final concentration of 0.66% and 13.0 M, respectively. Samples were incubated in a room temperature water bath for 30 min, and then transferred to a 96-well plate and the absorbance was measured at 482 nm on an Omega Star Microplate Reader (BMG LABTECH). Carbohydrate content was determined by linear regression using a standard curve of known glucose concentrations (range 0–3 mM).

Particulate Carbon and Nitrogen Analysis

Particulate organic carbon and particulate organic nitrogen were quantified using a particulate autoanalyzer (Costech Elemental Analyzer, Costech Analytical Technologies, Valencia, CA, USA) as described by Hutchins et al. (2002). Briefly, 5 mL of culture were filtered onto pre-combusted GF/F Whatman glass-fiber filters, stored at -80°C and dried in an 80°C oven prior to analysis. Phenylalanine and ethylenediaminetetraacetic acid were used as standards.

Photosynthetic Physiology

Cultures were filtered onto GF/A glass fiber filters and chlorophyll *a* (chl *a*) was extracted in 5 mL of 90% acetone for 24 h at −20°C. Chl *a* fluorescence was measured on a Turner 10-AU fluorometer. A 1 mL subsample of culture was held under low light conditions for 20 min and dark adapted for 2 min (Hennige et al., 2013), prior to measuring fluorescence with a Fast Repetition Rate Fluorometer (FRRf; Chelsea Technologies Group, West Molesey, UK). The following photosynthetic parameters were quantified (Cosgrove and Borowitzka, 2011): maximum photochemical efficiency of PSII (F_v/F_m), the functional absorption cross section of PSII (σ), energy transfer between PSII units (p), the time constant for reoxidation of Q_A acceptor in the PSII reaction center (τ), minimum fluorescence (F_o), and maximum (F_m) fluorescence.

FAME Analysis

Fatty acid methyl esters (FAMEs) were prepared by acid catalyzed direct transesterification (Ichihara and Fukubayashi, 2010). Briefly, the lyophilized cells were re-suspended in 0.2 mL toluene. Then 1.5 mL methanol and 0.3 mL 8% (w/v) HCl in methanol solution were added to the mixture. This solution was incubated at 45°C overnight. FAMEs were subsequently extracted in 1 mL hexane. Tridecanoic acid (C13:0; final concentration of 30.1 μM) was added as an internal standard. Extracted FAMEs were stored at -20°C until analysis. FAMEs were analyzed by gas chromatography on a Hewlett Packard HP 5890 Series equipped with a flame ionization detector and a Zebron ZB-Wax column (60 m × 0.32 mm × 0.25 μm, Phenomenex, Torrance, CA, USA). Supelco 37 component FAME mix (Sigma Aldrich, St. Louis, MO, USA) was used as a standard for fatty acid identification and quantification. FAMEs were resolved using splitless injection and heating the column as follows: initial oven temperature 190°C, increased by a 15°C/min to 250°C, and held at 250°C for 25 min.

Estimation of Biodiesel Parameters

The following equations were used to estimate saponification number (SN, Eq. 3), iodine number (IN, Eq. 4), and cetane

number (CN, Eq. 5) (Lei et al., 2012):

$$\mathrm{SN} = \sum (560 \times P_i) \div \mathrm{MW}_i \quad (3)$$

$$\mathrm{IN} = \sum (254 \times D \times P_i) \div \mathrm{MW}_i \quad (4)$$

$$\mathrm{CN} = 46.3 + 5458 \div \mathrm{SN} - 0.225 \times \mathrm{IN} \quad (5)$$

where P_i is the weight percent of each FAME, MW_i is the molecular weight of each FAME, and D is the number of double bonds in each FAME.

Statistical Analysis

Statistical analysis was performed using JMP Pro v11.2 software (SAS, Cary, NC, USA). Prior to comparison of means, data were assessed for normality and equality of variance. Raw data that did not meet assumptions of equal variance (by Levene's test) and/or normality (by the Kolmogorov-Smirnov test) were transformed prior to statistical analysis. Differences were determined to be statistically significant when $P < 0.05$.

For mean comparisons of total carbohydrate, protein and lipid content, lipid profiles, gene expression, seawater chemistry, particulate carbon and nitrogen, and photochemistry between air and simulated flue gas cultures, SDs were calculated from the average of replicates ($n = 4$) and means were compared using the Student's *t*-test. In cases where transformed data did not meet assumptions of equal variance and normality, the non-parametric Wilcoxon Rank-Sum test was used to compare means.

For mean comparisons of growth rate and maximum cell density between combinations of air, flue gas, 0 μM $NaNO_3$, and 220 μM $NaNO_3$, interaction effects were tested using a full factorial two-way ANOVA. There were no significant interaction effects for this dataset, so means were compared using a one-way ANOVA with Tukey HSD *post hoc* analysis.

Results

Carbon Chemistry

pH was significantly lower for flue gas (6.916 ± 0.037) versus air (7.336 ± 0.155) cultures ($P < 0.01$), which increased the proportion of dissolved CO_2 in the total DIC pool from 4.0% to 9.6% (**Table 1**). Flue gas treatment resulted in a large increase in both DIC and pCO_2 levels in cultures. Maximum pCO_2 levels in cultures treated with a model flue gas (12% CO_2) were 82-fold higher than cultures treated with atmospheric levels of CO_2.

Expression of *NR2-2/2HbN*

Relative expression of the *NR2-2/2HbN* transcript significantly differed between air grown cultures (1.4 ± 0.8) and flue gas cultures (6.2 ± 1.8), resulting in a 4.4-fold increase in transcript abundance in response to treatment conditions ($P < 0.02$).

Productivity

Total biomass productivity was significantly higher for flue gas cultures [18.2 (±2.6) mg L^{-1} day^{-1}] versus air cultures [7.0 (±1.9) mg L^{-1} day^{-1}, $P < 0.001$). In addition to an increase in growth rate, a significant increase in average cell diameter from 10.5 μm in air to 12.0 μm in flue gas cultures was also observed ($P < 0.03$). The effect of flue gas on the productivity of biochemical constituents varied (**Figure 1**). While there was a 13-fold increase in carbohydrate ($P < 0.001$) and a 2-fold increase in protein ($P < 0.001$), both total lipid productivity and cellular lipid composition (pg/cell basis, data not shown) were unaffected. Chlorophyll *a* content also increased in flue gas cultures compared to controls (1.09 ± 0.05 and 0.92 ± 0.09 pg/cell, respectively, $P < 0.001$). The simultaneous increase in both carbohydrates and proteins was reflected in the maintenance of C:N ratios between air (7.2 ± 0.7) and flue gas (7.8 ± 0.9) cultures.

TABLE 1 | Carbon chemistry of *Heterosigma akashiwo* cultures bubbled with air (control) or a simulated flue gas containing 12% CO_2 and 150 ppm NO.

	Air	Flue Gas
DIC (μM)	223 (±53)	7767 (±259)
pCO_2 (μatm)	282 (±112)	23,247 (±1317)
HCO_3^- (μmol/kg SW)	210 (±49)	6980 (±276)
CO_3^{2-} (μmol/kg SW)	3 (±1)	38 (±5)
CO_2 (μmol/kg SW)	9 (±4)	748 (±42)

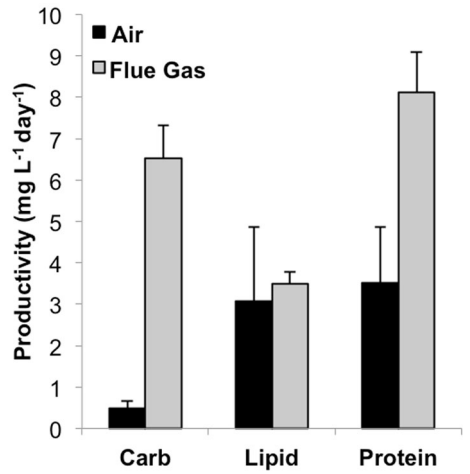

FIGURE 1 | Carbohydrate, lipid, and protein productivity for *Heterosigma akashiwo* bubbled with air (control) or simulated flue gas containing 12% CO_2 and 150 ppm NO. Data plotted are mean values ± SD ($n = 4$).

Photosynthetic Physiology

Dark-adapted photosynthetic measurements are summarized in **Table 2**. Maximum photochemical efficiency of PSII (F_v/F_m) and the rate of PSII re-oxidation (t) were both significantly lower in flue gas cultures ($P < 0.001$), while the functional absorption cross section (S_{PSII}) did not change in response to flue gas. Both minimum (F_o) and maximum (F_m) raw fluorescence significantly increased in flue gas cultures ($P < 0.001$), which coincided with a significant increase in chl *a* content as previously noted.

FAME Analysis

The following fatty acids were the predominant constituents in all growth conditions: C18:4, C16:0, C20:5n3, and C16:1. In

TABLE 2 | Maximum photochemical efficiency of PSII (F_v/F_m), functional absorption cross section (S_{PSII}), rate of PSII re-oxidation (t), minimum (F_o) and maximum (F_m) fluorescence measured in the dark for *Heterosigma akashiwo* grown on air (control) or simulated flue gas (treatment).

	Air	Flue Gas
F_v/F_m	0.498 (±0.009)	0.458 (±0.002)
S_{PSII} (Å^2 quantum^{-1})	1.10 (±0.03)	1.10 (±0.02)
t (μs)	708 (±8)	621 (±20)
F_o (RFU)	6144 (±1)	11,758 (±1)
F_m (RFU)	12,250 (±1)	21,764 (±1)

Error represents SD (n = 4).

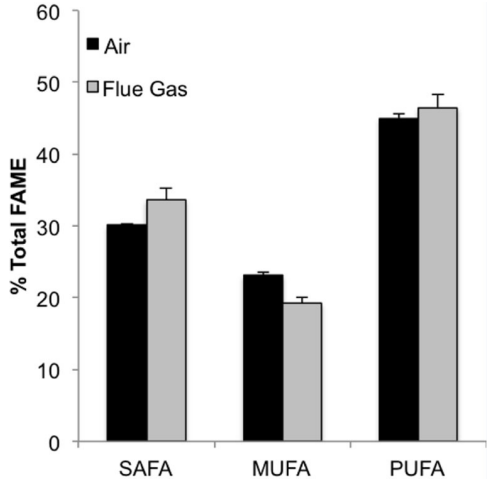

FIGURE 2 | Classification of fatty acid saturation as a percentage of total fatty acid methyl esters (FAMEs) for *Heterosigma akashiwo* bubbled with air (control) or simulated flue gas containing 12% CO_2 and 150 ppm NO. SAFA, saturated fatty acids; MUFA, monounsaturated fatty acids; PUFA, polyunsaturated fatty acids. Data plotted are mean values ± SD ($n = 4$).

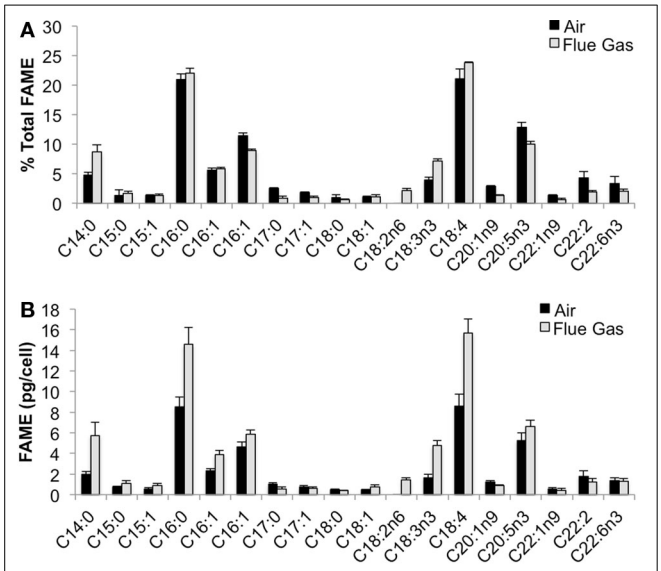

FIGURE 3 | Fatty acid methyl ester (FAME) profile for *Heterosigma akashiwo* bubbled with air (control) or simulated flue gas containing 12% CO_2 and 150 ppm NO. (**A**) Individual FAMEs are reported as mean percent of total FAMEs ± SD ($n = 4$). (**B**) Individual FAMEs are reported on a per cell basis as mean pg/cell ± SD ($n = 4$).

TABLE 3 | Calculated values for estimated biodiesel quality based on FAME profiles for *Heterosigma akashiwo* grown on air (control) or simulated flue gas (treatment).

	Pre-extraction		Post-extraction (70%)		Post-extraction (100%)	
	Air	Flue gas	Air	Flue gas	Air	Flue gas
SN	197 (±1)	200 (±1)	178 (±2)	185 (±2)	170 (±2)	179 (±2)
IN	177 (±4)	175 (±5)	133 (±4)	141 (±2)	114 (±5)	126 (±1)
CN	34 (±1)	34 (±1)	47 (±1)	44 (±0.2)	53 (±2)	48 (±0.1)

SN, saponification number; IN, iodine number; CN, cetane number were calculated for biomass under three scenarios: without EPA/DHA extraction, with 70% extraction recovery of EPA/DHA, and with total recovery of EPA/DHA. Error represents SD (n = 4).

response to flue gas, the proportion of saturated fatty acids (SAFA) significantly increased ($P < 0.01$), the proportion of mono-unsaturated fatty acids (MUFA) significantly declined ($P < 0.001$), while the proportion of polyunsaturated fatty acids (PUFA) remained constant (**Figure 2**). The proportional composition of individual FAMEs in the total FAME pool showed that the significant increase in total SAFA was driven by a 1.8-fold increase in C14:0 ($P < 0.001$; **Figure 3A**). Conversely, the significant decrease in total MUFA was attributable to a decline in C17:1 and C22:1n9 ($P < 0.02$ in both cases). Total PUFA remained constant due to balanced increases and decreases in several individual PUFAs. Notably, the presence of C18:2n6 was only detected at a low concentration in one air (control) replicate, but represented 2.2 (± 0.3)% of total FAMEs in response to flue gas. In addition, the proportion of C18:4 also increased in response to flue gas ($P < 0.05$) while both C20:5n3 and C22:2 declined ($P < 0.005$ and $P < 0.04$, respectively).

When FAMEs are plotted on a cellular basis, additional patterns emerged (**Figure 3B**). The predominant fatty acids (C18:4, C16:0, C20:5n3, and C16:1) are all significantly increased on a per cell basis in response to flue gas. There was a 1.83-fold increase in C18:4 ($P < 0.001$), a 1.70-fold increase in C16:0 ($P < 0.002$), a 1.25-fold increase in C20:5n3 ($P < 0.05$), and a total 1.97-fold increase in total isomers of C16:1 ($P < 0.01$).

Estimation of Biodiesel Parameters

Calculated values for estimated biodiesel quality are summarized in **Table 3**. Both air and flue gas cultures have an estimated cetane number (CN) of 34. Eicosapentaenoic acid (EPA) and docosahexaenoic acid (DHA) are long chain, polyunsaturated fatty acids, and their presence resulted in high estimated saponification number (SN) and iodine number (IN) values, which contributed to a decrease in estimated CN. Therefore, CN was also calculated after extraction of EPA/DHA.

Effect of Nitrate Levels on Growth in Air Versus Simulated Flue Gas

Figure 4 summarizes specific growth rate (μ) and maximum cell density (cells/mL) achieved in cultures grown under the following

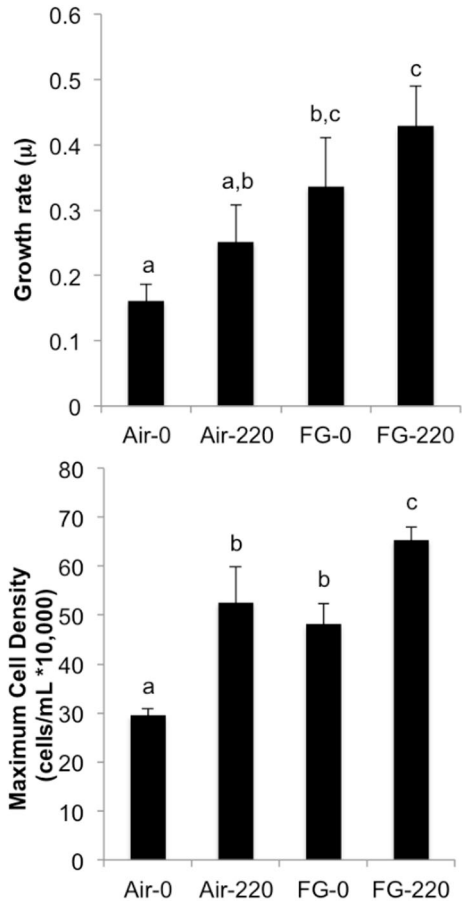

FIGURE 4 | Specific growth rate (μ) and maximum cell density (cells/mL) for cultures grown under the following conditions: air and 0 μM $NaNO_3$ (Air-0), air and 220 μM $NaNO_3$ (Air-220), flue gas and 0 μM $NaNO_3$ (FG-0), and flue gas and 220 μM $NaNO_3$ (FG-220). Data plotted are mean values ± SD ($n = 4$). Letters denote significant differences at the $P < 0.05$ level.

conditions: air and 0 μM $NaNO_3$ (Air-0), air and 220 μM $NaNO_3$ (Air-220), flue gas and 0 μM $NaNO_3$ (FG-0), and flue gas and 220 μM $NaNO_3$ (FG-220). There was not a significant interaction effect of gas type and nitrate concentration on growth rate or maximum cell density. FG-0 grew at the same rate as both Air-220 and FG-220 cultures. All cultures grew faster than Air-0, which was observed to be the only treatment to form resting cysts during stationary phase. FG-220 achieved the highest maximum cell density, while maximum cell densities for FG-0 and Air-220 were not significantly different.

Discussion

Growth on a simulated flue gas with relevant NOx levels more than doubled the biomass productivity of *H. akashiwo*. Flue gas treatment drastically increased the amount of bioavailable carbon in the media (**Table 1**), and the accumulation of large amounts of storage carbohydrates suggests that *Heterosigma* is effective at fixing this excess CO_2. Maintenance of the C:N ratio along with an increase in protein content suggests that CO_2 assimilation in flue gas cultures was not limited by nitrogen availability. Photochemical measurements also indicated that photosynthesis in *Heterosigma* is not inhibited by high CO_2 and NO concentrations (**Table 2**). For example, the rate of PSII re-oxidation (t) was 87 μs faster, suggesting that photosynthetic electron transport was enhanced during growth on flue gas and that cells maintained overall photosynthetic efficiency despite an observed decline in dark-acclimated F_v/F_m. Growth rates and maximum cell densities of *Heterosigma* grown on simulated flue gas without supplemental nitrogen (FG-0) demonstrated that nitrogen derived from NO gas is biologically available to support enhanced CO_2 fixation (**Figure 4**). In addition, the increase in *NR2-2/2HbN* transcript abundance observed here supports the hypothesis that this chimeric enzyme is involved in maintaining cell growth in the presence of NO (Stewart and Coyne, 2011). Collectively, these results support the hypothesis that *Heterosigma* is an ideal candidate for the commercial production of algal biomass using industrial emissions containing high levels of CO_2 and NO.

Heterosigma biomass was subsequently analyzed for its potential to become a biofuel feedstock. In the conventional algae to biofuel pathway, algal lipids are extracted and upgraded to biodiesel (Davis et al., 2012). The residual biomass, which accounts for 50–75% of the total biomass, is then processed into non-fuel products, such as animal feeds and high value chemicals, or is subjected to anaerobic digestion (Davis et al., 2012). In the present study, growth on simulated flue gas did not reduce total lipid yields, so changes in lipid profiles were investigated to assess the potential for converting this lipid fraction to quality biodiesel. The American Society for Testing and Materials standards specify that the CN must be a minimum of 47 for B100 biodiesel and a minimum of 40 for blended B6 to B20 biodiesels (ASTM International, 2014). CNs based on total lipid composition for both air and flue gas cultures were well below this standard unless at least 70% of EPA/DHA was theoretically extracted prior to the transesterification of lipids (**Table 3**). The omega-3 fatty acids, eicosapentaenoic acid (EPA, C20:5n3) and docosahexaenoic acid (DHA, C22:6n3), are potential value-added products from this species with an estimated bulk wholesale value of $12,540/kg for >70% pure oil (J Edwards International, Inc., personal communication). In this study, EPA and DHA constituted approximately 12–16% of total FAMEs. Since the removal of these polyunsaturated fatty acids from the lipid mixture before conversion to biodiesel also enhances the quality of the resulting fuel, purification of these lipids prior to further processing could be economically feasible (Molina Grima et al., 2003; Chauton et al., 2014).

Interestingly, the predominant fatty acids profiled here (C18:4, C16:0, C20:5n3, and C16:1) are the main fatty acyl substituents of the thylakoid sulfolipid, sulfoquinovosyl diacylglycerol (SQDG), which is produced at high levels in *Heterosigma* (Keusgen et al., 1997). Enhanced synthesis of these fatty acids in the presence of high CO_2 and NO (**Figure 3**) likely functioned to support an increase in thylakoid number or surface area as suggested by a significant 17% increase in chlorophyll content (Benning, 1998; Minoda et al., 2002). This subsequently explains the increase in C14:0, which is linked to the fatty acid synthase enzyme prior to the two carbon elongation cycle that produces C16:0,

where C16:0 is then released from fatty acid synthase as the precursor to long chain saturated and unsaturated fatty acid synthesis. Here, it appears that changes in individual fatty acid content on a cellular basis were driven by photosynthetic requirements.

In this study, lipid production did not benefit from growth on flue gas, whereas carbohydrate and protein output was significantly enhanced. A recent advancement in algal biomass processing provides an alternative to focusing solely on lipids as the primary feedstock for biofuel production. Whole algae hydrothermal liquefaction can produce fuels using the entire biomass in lieu of separating its biochemical components and has been characterized as a technically and economically feasible processing scheme (Biddy et al., 2013). Under this scheme, the primary goal is to maximize overall biomass productivity, with increases in growth rates and/or increases in the storage of any cellular product contributing to the target outcome. With hydrothermal liquefaction, the large increase in carbohydrates and protein in response to flue gas observed in the present study (**Figure 1**) is advantageous for increasing total biofuel yields. In contrast to green algae, *Heterosigma* stores photosynthetic energy not only in the form of lipids, but also as water-soluble carbohydrates stored within vacuoles (Chiovitti et al., 2006), and the dramatic increase in carbohydrates seen here indicates that *Heterosigma* is metabolically suited to fix large amounts of anthropogenic CO_2 into valuable biomass. Together, these results illustrate the robustness of this alga and support continued efforts to assess the viability of this species for commercial-scale biomass production and bioremediation of industrial emissions.

Acknowledgments

This work was supported by the United States Department of Agriculture (USDA-NIFA-2011-67012-31175 to JS), the National Oceanic and Atmospheric Administration through Delaware Sea Grant (Award #NA10OAR4170084-12 to JS and KC and Award #NA14OAR4170087 to JS and KC), and the National Science Foundation (Award #1314003 to JS). We would like to acknowledge Catherine Fitzgerald at Salisbury University for her assistance in developing the GC protocol for the resolution of long chain FAMEs. We would also like to thank Mark Warner (University of Delaware) and Josée Nina Bouchard (Algenol, Fort Myers, FL, USA) for technical support.

References

ASTM International. (2014). *Standard Specification for Biodiesel Fuel Blend Stock (B100) for Middle Distillate Fuels: Designation D6751-14*. West Conshohocken, PA: ASTM International.

Basu, S., Roy, A. S., Mohanty, K., and Ghoshal, A. K. (2013). Enhanced CO_2 sequestration by a novel microalga: *Scenedesmus obliquus* SA1 isolated from bio-diversity hotspot region of Assam, India. *Bioresour. Technol.* 143, 369–377. doi:10.1016/j.biortech.2013.06.010

Benemann, J. (2013). Microalgae for biofuels and animal feeds. *Energies* 6, 5869–5886. doi:10.3390/en6115869

Benning, C. (1998). Biosynthesis and function of the sulfolipid sulfoquinovosyl diacylglycerol. *Annu. Rev. Plant Physiol. Plant Mol. Biol.* 49, 53–75. doi:10.1146/annurev.arplant.49.1.53

Biddy, D., Jones, R., Zhu, S., Bilal, K; Pacific Northwest National Laboratory, and National Renewable Energy Laboratory. (2013). *Whole Algae Hydrothermal Liquefaction Technology Pathway: Technical Report* NREL/TP-5100-58051. Washington, DC: U.S. Department of Energy.

Borkenstein, C. G., Knoblechner, J., Frühwirth, H., and Schagerl, M. (2011). Cultivation of *Chlorella emersonii* with flue gas derived from a cement plant. *J. Appl. Phycol.* 23, 131–135. doi:10.1007/s10811-010-9551-5

Chauton, M. S., Reitan, K. I., Norsker, N. H., Tveterås, R., and Kleivdal, H. T. (2014). A techno-economic analysis of industrial production of marine microalgae as a source of EPA and DHA-rich raw material for aquafeed: research challenges and possibilities. *Aquaculture* 436, 95–103. doi:10.1016/j.aquaculture.2014.10.038

Chen, H. W., Yang, T. S., Chen, M. J., Chang, Y. C., Lin, C. Y., Wang, E. I., et al. (2012). Application of power plant flue gas in a photobioreactor to grow *Spirulina* algae, and a bioactivity analysis of the algal water-soluble polysaccharides. *Bioresour. Technol.* 120, 256–263. doi:10.1016/j.biortech.2012.04.106

Cheng, Y., Zheng, Y., and VanderGheynst, J. S. (2011). Rapid quantitative analysis of lipids using a colorimetric method in a microplate format. *Lipids* 46, 95–103. doi:10.1007/s11745-010-3494-0

Chiovitti, A., Ngoh, J. E., and Wetherbee, R. (2006). 1, 3-β-d-glucans from *Haramonas dimorpha* (Raphidophyceae). *Botanica Marina* 49, 360–362. doi:10.1515/BOT.2006.045

Chiu, S. Y., Kao, C. Y., Huang, T. T., Lin, C. J., Ong, S. C., Chen, C. D., et al. (2011). Microalgal biomass production and on-site bioremediation of carbon dioxide, nitrogen oxide and sulfur dioxide from flue gas using *Chlorella* sp. cultures. *Bioresour. Technol.* 102, 9135–9142. doi:10.1016/j.biortech.2011.06.091

Cosgrove, J., and Borowitzka, M. A. (2011). "Chlorophyll fluorescence terminology: an introduction," in *Chlorophyll a Fluorescence in Aquatic Sciences: Methods and Applications*, eds D. J. Suggett, O. Prasil, and M. A. Borowitzka (New York, NY: Springer), 1–18.

Coyne, K. J., and Cary, S. C. (2005). Molecular approaches to the investigation of viable dinoflagellate cysts in natural sediments from estuarine environments. *J. Euk. Microbiol.* 52, 90–94. doi:10.1111/j.1550-7408.2005.05202001.x

Davis, R., Fishman, D., Frank, E. D., Wigmosta, M. S., et al. (2012). *Renewable Diesel from Algal Lipids: An Integrated Baseline for Cost, Emissions, and Resource Potential from a Harmonized Model. NREL/TP-5100-55431*. Washington, DC: U.S. Department of Energy.

Dickson, A. G. (1990). Standard potential of the reaction – AGCL(S)+1/2H-2(G)=AG(S)+HCL(AQ) and the standard acidity constant of the ion HSO4- in synthetic sea-water from 273.15-k to 318.15-k. *J. Chem. Thermodyn.* 22, 113–127. doi:10.1016/0021-9614(90)90074-Z

Doucha, J., Straka, F., and Lívanský, K. (2005). Utilization of flue gas for cultivation of microalgae *Chlorella* sp. in an outdoor open thin-layer photobioreactor. *J. Appl. Phycol.* 17, 403–412. doi:10.1007/s10811-005-8701-7

Douskova, I., Doucha, J., Livansky, K., Machat, J., Novak, P., Umysova, D., et al. (2009). Simultaneous flue gas bioremediation and reduction of microalgal biomass production costs. *Appl. Microbiol. Biotechnol.* 82, 179–185. doi:10.1007/s00253-008-1811-9

Dubois, M., Gilles, K., Hamilton, J., Rebers, P., and Smith, F. (1956). Colorimetric method for determination of sugars and related substances. *Anal. Chem.* 28, 350–356. doi:10.1021/ac60111a017

EPA. (2012). *Overview of Greenhouse Gases: Carbon Dioxide Emissions*. Available at: http://www.epa.gov/climatechange/ghgemissions/gases/co2.html

EPA. (2014). *Ground Level Ozone: Basic Information*. Available at: http://www.epa.gov/climatechange/ghgemissions/gases/co2.html

Folch, J., Lees, M., Stanley, G. H. S., Han, J. I., and Park, J. K. (1957). A simple method for the isolation and purification of total lipids from animal tissues. *J. Biol. Chem.* 226, 497–509.

Friederich, G. E., Walz, P. M., Burczynski, M. G., and Chavez, F. P. (2002). Inorganic carbon in the central California upwelling system during the 1997 – 1999 el niño – la niña event. *Prog. Oceanogr.* 54, 185–203. doi:10.1016/S0079-6611(02)00049-6

Fuentes-Grünewald, C., Garcés, E., Alacid, E., Rossi, S., and Camp, J. (2013). Biomass and lipid production of dinoflagellates and raphidophytes in indoor and outdoor photobioreactors. *Mar. Biotechnol.* 15, 37–47. doi:10.1007/s10126-012-9450-7

Fuentes-Grünewald, C., Garcés, E., Alacid, E., Sampedro, N., Rossi, S., and Camp, J. (2012). Improvement of lipid production in the marine strains *Alexandrium minutum* and *Heterosigma akashiwo* by utilizing abiotic parameters. *J. Ind. Microbiol. Biotechnol.* 39, 207–216. doi:10.1007/s10295-011-1016-6

Fuentes-Grünewald, C., Garcés, E., Rossi, S., and Camp, J. (2009). Use of the dinoflagellate *Karlodinium veneficum* as a sustainable source of biodiesel production. *J. Ind. Microbiol. Biotechnol.* 36, 1215–1224. doi:10.1007/s10295-009-0602-3

Guillard, R. R. L. (1975). "Culture of phytoplankton for feeding marine invertebrates," in *Culture of Marine Invertebrate Animals*, eds W. L. Smith and M. H. Chanley (New York, NY: Plenum Press), 26–60.

Hara, Y., and Chihara, C. (1987). Morphology, ultrastructure and taxonomy of the raphidophycean alga, *Heterosigma akashiwo*. *Bot. Mag.* 100, 151–163. doi:10.1007/BF02488320

Harter, T., Bossier, P., Verreth, J. A. J., Bode, S., van der Ha, D., Deebeer, A. E., et al. (2013). Carbon and nitrogen mass balance during flue gas treatment with *Dunaliella salina* cultures. *J. Appl. Phycol.* 25, 359–368. doi:10.1007/s10811-012-9870-9

Hennige, S. J., Coyne, K. J., Macintyre, H., Liefer, J., and Warner, M. E. (2013). The photobiology of *Heterosigma akashiwo*: photoacclimation, diurnal periodicity, and its ability to rapidly exploit exposure to high light. *J. Phycol.* 49, 349–360. doi:10.1111/jpy.12043

Hutchins, D. A., Hare, C. E., Weaver, R. S., Zhang, Y., Firme, G. F., DiTullio, G. R., et al. (2002). Phytoplankton iron limitation in the Humboldt current and Peru upwelling. *Limnol. Oceanogr.* 47, 997–1011. doi:10.4319/lo.2002.47.4.0997

Ichihara, K., and Fukubayashi, Y. (2010). Preparation of fatty acid methyl esters for gas-liquid chromatography. *J. Lipid Res.* 51, 635–640. doi:10.1194/jlr.D001065

Jiang, Y., Zhang, W., Wang, J., Chen, Y., Shen, S., and Liu, T. (2013). Utilization of simulated flue gas for cultivation of *Scenedesmus dimorphus*. *Bioresour. Technol.* 128, 359–364. doi:10.1016/j.biortech.2012.10.119

Jin, H. F., Santiago, D. E. O., Park, J., and Lee, K. (2008). Enhancement of nitric oxide solubility using Fe(II)EDTA and its removal by green algae *Scenedesmus* sp. *Biotechnol. Bioprocess Eng.* 13, 48–52. doi:10.1007/s12257-007-0164-z

Keusgen, M., Curtis, J. M., Thibault, P., Walter, J. A., Windust, A., and Ayer, S. W. (1997). Sulfoquinovosyl diacylglycerols from the alga *Heterosigma carterae*. *Lipids* 32, 1101–1112. doi:10.1007/s11745-997-0142-9

Lara-Gil, J. A., Álvarez, M. M., and Pacheco, A. (2014). Toxicity of flue gas components from cement plants in microalgae CO_2 mitigation systems. *J. Appl. Phycol.* 26, 357–368. doi:10.1007/s10811-013-0136-y

Lei, A., Chen, H., Shen, G., Hu, Z., Chen, L., and Wang, J. (2012). Expression of fatty acid synthesis genes and fatty acid accumulation in *Haematococcus pluvialis* under different stressors. *Biotechnol. Biofuels* 5, 1–11. doi:10.1186/1754-6834-5-18

Li, Y. H., Takahash, T., and Broecker, W. S. (1969). Degree of saturation of CACO3 in oceans. *J. Geophys. Res.* 74, 5507. doi:10.1371/journal.pone.0016069

Martínez, R., Orive, E., Laza-Martínez, A., and Seoane, S. (2010). Growth response of six strains of *Heterosigma akashiw*o to varying temperature, salinity and irradiance conditions. *J. Plankton Res.* 32, 529–538. doi:10.1093/plankt/fbp135

Minoda, A., Sato, N., Nozaki, H., Okada, K., Takahashi, H., Sonoike, K., et al. (2002). Role of sulfoquinovosyl diacylglycerol for the maintenance of photosystem II in *Chlamydomonas reinhardtii*. *Eur. J. Biochem.* 269, 2353–2358. doi:10.1046/j.1432-1033.2002.02896.x

Molina Grima, E., Belarbi, E. H., Acién Fernández, F. G., Robles Medina, A., and Chisti, Y. (2003). Recovery of microalgal biomass and metabolites: process options and economics. *Biotechnol. Adv.* 20, 491–515. doi:10.1016/S0734-9750(02)00050-2

Nagarajan, S., Chou, S. K., Cao, S., Wu, C., and Zhou, Z. (2013). An updated comprehensive techno-economic analysis of algae biodiesel. *Bioresour. Technol.* 145, 150–156. doi:10.1016/j.biortech.2012.11.108

Santiago, D. E. O., Jin, H. F., and Lee, K. (2010). The influence of ferrous-complexed EDTA as a solubilization agent and its auto-regeneration on the removal of nitric oxide gas through the culture of green alga *Scenedesmus* sp. *Process Biochem.* 45, 1949–1953. doi:10.1016/j.procbio.2010.04.003

Sharp, J. H., Yoshiyama, K., Parker, A. E., Schwartz, M. C., Curless, S. E., Beauregard, A. Y., et al. (2009). A biogeochemical view of estuarine eutrophication: seasonal and spatial trends and correlations in the Delaware estuary. *Estuaries Coast.* 32, 1023–1043. doi:10.1007/s12237-009-9210-8

Stewart, J. J., and Coyne, K. J. (2011). Analysis of raphidophyte assimilatory nitrate reductase reveals unique domain architecture incorporating a 2/2 hemoglobin. *Plant Mol. Biol.* 77, 565–575. doi:10.1007/s11103-011-9831-8

Wilson, M. H., Groppo, J., Placido, A., Graham, S., Morton, S. A. III, Santillan-Jimenez, E., et al. (2014). CO_2 recycling using microalgae for the production of fuels. *Appl. Petrochem. Res.* 4, 41–53. doi:10.1007/s00253-012-4362-z

Zhang, Y., Fu, F.-X., Whereat, E., Coyne, K. J., and Hutchins, D. A. (2006). Bottom-up controls on a mixed-species HAB assemblage: a comparison of sympatric *Chattonella subsalsa* and *Heterosigma akashiwo* (Raphidophyceae) isolates from the Delaware Inland Bays, USA. *Harmful Algae* 5, 310–320. doi:10.1016/j.hal.2005.09.001

Conflict of Interest Statement: Jennifer J. Stewart and Kathryn J. Coyne. (2013). Novel Nitrate Reductase Fusion Proteins and Uses Thereof. U.S. Patent No. 8,409,827. Washington, DC: U. S. Patent and Trademark Office. The other co-authors declare that the research was conducted in the absence of any commercial or financial relationships that could be construed as a potential conflict of interest.